Geophys. J. Int. (2003) **155,** 1006–1020

An anisotropic fractured poroelastic effective medium theory

S. R. Tod[1,2,*]

[1]*Department of Applied Mathematics and Theoretical Physics, Centre for Mathematical Sciences, Wilberforce Road, Cambridge* CB3 0WA, *UK. E-mail: S.R.Tod@damtp.cam.ac.uk*
[2]*British Geological Survey, West Mains Road, Edinburgh* EH9 3LA, *UK*

Accepted 2003 August 12. Received 2003 July 9; in original form 2002 September 19

SUMMARY

Effective medium theories are used to describe the overall properties of a material containing cracks that are on a scale length much less than a wavelength, during the propagation of seismic waves. These theories are in general derived for an elastic medium with or without some form of fluid connection between the cracks. The theories are adequate for describing the properties of a material with low matrix porosities, such as carbonates, but provide a poor approximation once the matrix porosity has increased sufficiently to play an important role in determining the material properties of the effective medium, such as in sandstones. The behaviour of wave propagation within a poroelastic medium differs significantly from that in a purely elastic medium. To this end, a poroelastic model is required. Assuming that the saturated matrix material can be described by Biot's equations of poroelasticity, the method of smoothing can be used to develop an effective medium theory to first order in crack volume density in much the same way as Hudson theory uses the method for an elastic medium; the cracks are assumed to be on a scale much greater than the microscale that describes the porous matrix and much less than the macroscale, characterized by the wavelength of propagating waves. By this approach we derive effective poroelastic constants for a matrix permeated with ellipsoidal inclusions of a differing material, where the whole system is saturated with a single fluid.

Key words: anisotropy, attenuation, cracked media, Green's functions, poroelasticity, porosity.

1 INTRODUCTION

The interpretation of anisotropy measurements made from seismic reflection data requires a theoretical model that allows for the relation of material parameters to macroscopically determined properties (e.g. Thomsen 1995). The regions of interest, areas of oil and gas reserves, are frequently influenced by fractures, or cracks, with a range of scale lengths (Yielding *et al.* 1992). On the assumption that the scale length associated with the fracturing is considerably smaller than that of the seismic wavelength, a description of the average properties of a medium will suffice; the mean wave should provide a good approximation to the observed wave, and scattering can be largely ignored. Of interest then are the properties of the resulting effective medium.

Effective medium theories have been developed using a number of different techniques (e.g. O'Connell & Budiansky 1974; Hudson 1980; Nishizawa 1982) to provide a description of an elastic medium containing fractures or cracks, in a long-wavelength, low-crack-density limit. The cracks may contain a range of material infills (Hudson 1981) and may be isolated or connected via some fluid flow mechanism (Mavko & Nur 1975; Thomsen 1995; Hudson *et al.* 1996). These models may be sufficient for providing an effective description of a material with a low matrix porosity, such as carbonates, but become inadequate once the matrix porosity is large enough to play a significant role in determining the effective behaviour of the medium, such as sandstones. Attempts have been made to increase the range of porosities over which the theories are valid (Berge *et al.* 1992). However, these do not go far enough. A poroelastic description is then required. The behaviour of a poroelastic medium is significantly different from that of a purely elastic one.

While porosity in the Earth can take many forms, there are only two types that are of importance at the scale of the reservoir; large-volume, low-permeability 'storage' porosity associated with the reservoir and low-volume, high-permeability 'transport' porosity associated with the cracks that provides pathways for fluid to escape from the reservoir and is the key to reservoir analysis and the economics of fluid withdrawal.

*Now at: BP Exploration Operating Co. Ltd, Chertsey Road, Sunbury on Thames, Middlesex TW16 7LN, UK. E-mail: tods01@bp.com

A macroscopic description of fluid-filled porous media was first developed by Biot (1941) and Gassmann (1951a,b). Biot derived his description by superposing two interacting macroscopic continua, the solid and fluid phases, rather than by starting with the governing equations of the microscopically separate components. Biot's theory predicts the existence of a second, slow, compressional wave. Plona (1980) was the first to observe this experimentally in synthetic sandstone, and Kelder & Smeulders (1997) observed the phenomena in naturally occurring rock. The results of Gassmann (1951b) were extended to anisotropic media by Brown & Korringa (1975) while Zimmerman (2000) describes the similarities that exist between Biot's equations of poroelasticity and the equations of thermoelasticity. There is, however, experimental evidence that disagrees with the predictions of Biot theory (Winkler 1985; Gist 1994) suggesting that there must be additional factors, such as fractures, contributing to the attenuation of waves.

More recently, attempts to connect the microstructural behaviour with the macroscopic description have been developed using two-scale homogenization techniques (Levy 1979; Auriault 1980; Burridge & Keller 1981) that assume the ratio between the length-scales associated with the microstructure, l, and macroscopic properties, L, is small. That is, $\epsilon = l/L \ll 1$. At the microscale the fluid is governed by the linearized Navier–Stokes equations—which relies on the fact that the characteristic timescale of the problem, ω^{-1}, is $\mathcal{O}(\epsilon)$ smaller than the ratio of the macroscopic length L and characteristic fluid velocity ωl—and the solid by the equations of linear elasticity, with a suitable choice of boundary conditions applied at the juncture of the two phases. The process is assumed to be isothermal. Provided a separation of scales is evident in the physical quantities (Auriault 1991), the equations are normalized and a matched asymptotic expansion is performed, leading to a set of governing equations for the averaged quantities, on the assumption that the medium is macroscopically uniform. Under certain conditions, Biot-like equations are recovered. A volume averaging technique (de la Cruz & Spanos 1985; Pride *et al.* 1992) similarly leads to Biot-like equations and de la Cruz & Spanos (1989) argue the need to include thermomechanical coupling effects, introducing non-linearities into the resulting governing equations. Le Ravalec & Guéguen (1994) also provide a thermoporoelastic description. Network-, or lattice-, based models have been developed by a number of authors, including Seeburger & Nur (1984) and Chapman *et al.* (2002), while Le Ravalec & Guéguen (1996) and Endres & Knight (1997) develop models for describing porosity in terms of an isotropic distribution of spheroids over a range of scales.

The form of the governing equations achieved via homogenization depends on the relative magnitude of the fluid viscosity and the elastic modulus of the porous matrix, $R = \|\boldsymbol{c}\|/\omega\eta_{\mathrm{f}}$, where $\|\boldsymbol{c}\|$ is an *a priori* estimate of the porous matrix elastic modulus, ω is frequency and η_{f} the fluid viscosity. Auriault & Royer (2002) classify the four alternative regimes that may be achieved for a single-porosity media; an empty elastic porous medium $R \leq \mathcal{O}(\epsilon^{-3})$, Biot's model $R = \mathcal{O}(\epsilon^{-2})$, an impermeable saturated porous matrix $R = \mathcal{O}(\epsilon^{-1})$ and a viscoelastic medium $R = \mathcal{O}(1)$. It is at $R = \mathcal{O}(\epsilon^{-2})$ that most interaction occurs between the fluid and solid phases and this is the regime of greatest interest. It is the only one of the four regimes that can be classed as a two-phase rather than a single-phase model.

Into the background of a porous medium we wish to distribute a set of fractures, yielding what is, in effect, a dual-porosity medium, where $l \ll a \ll L$ and l, a and L are scale lengths associated with the microscale, fractures and wavelength, respectively. The problem was first considered by Barenblatt *et al.* (1960). A three-scale homogenization method has been employed (Auriault & Boutin 1992, 1993, 1994) with a number of alternative models resulting, dependent upon the relative size of the two scale ratios. In contrast, Berryman & Wang (2000) use a phenomenological approach similar to the original Biot equations (Biot 1941), whereas Aifantis (1980) and Wilson & Aifantis (1984) use an idea of 'multiporosity'.

However, none of these models incorporate the shape of the crack. Berryman (1986) uses a self-consistent method to derive an effective medium approximation from the formulae for the scattering of a compressional wave from an inhomogeneous sphere (Berryman 1985). A generalization of the Eshelby (1957) work to poroelastic media (Berryman 1997) is incorporated into a number of effective medium theories by Berryman (1998). However, the work of Berryman (1998) is somewhat incomplete as it fails to provide effective values of all poroelastic parameters and provides no mention of anisotropy. It is with this in mind that we choose to follow the method of smoothing (Keller 1964), as used so successfully by Hudson (1980, 1981, 1994) for an elastic medium, to derive the effective poroelastic constants for a set of aligned ellipsoidal cracks within an otherwise isotropic, homogeneous, poroelastic background. Following Auriault & Royer (2002), we consider the two-phase model when homogenization theory reduces to the original equations of Biot.

The resulting anisotropic poroelastic effective medium theory exhibits the same form as the work of Biot (1955) and Cheng (1997), and furthermore, the deviation of the effective medium parameters from the isotropic background result is given explicitly in terms of the shape, orientation and material properties of the inclusions. The theory has the potential to be used in conjunction with laboratory experiments to help characterize rock parameters (Rasolofosaon & Zinszner 2002) and with reflection data to aid the understanding of the seismic properties of pore fluids (Batzle & Wang 1992). Indeed, the theory may provide a mechanism for explaining some of the discrepancies between theory and experiment in poroelasticity (e.g. Winkler 1985; Berryman & Wang 2001; King & Marsden 2002).

2 THE EQUATIONS OF MOTION

On the microscopic scale the equations of motion consist of those for the solid component, those for the fluid and boundary conditions between the two. Elastodynamics in the solid component gives stress $\boldsymbol{\tau}$ in terms of strain $\boldsymbol{e}$:

$$\boldsymbol{\tau} = \boldsymbol{c} : \boldsymbol{e}, \tag{1}$$

where the : denotes a two-index contraction between the tensors, and a momentum balance

$$\nabla \cdot \boldsymbol{\tau} = \rho_{\mathrm{s}} \ddot{\mathbf{u}}, \tag{2}$$

in terms of displacement **u**. Linearized compressible Navier–Stokes theory within the fluid gives stress $\boldsymbol{\sigma}$ in terms of pressure p and velocity **v**

$$\boldsymbol{\sigma} = -p\boldsymbol{I} + \eta_{\mathrm{f}}[\nabla\mathbf{v} + (\nabla\mathbf{v})^{\mathrm{T}} - 2\boldsymbol{I}\nabla\cdot\mathbf{v}/3], \tag{3}$$

a momentum balance:

$$\nabla\cdot\boldsymbol{\sigma} = \rho_{\mathrm{f}}\dot{\mathbf{v}} \tag{4}$$

and the isothermal compressibility relation

$$\dot{p} = -\kappa_{\mathrm{f}}\nabla\cdot\mathbf{v}, \tag{5}$$

while at the fluid–solid boundary

$$\mathbf{n}\cdot\boldsymbol{\sigma} = \mathbf{n}\cdot\boldsymbol{\tau}, \tag{6}$$

and

$$\mathbf{v} = \dot{\mathbf{u}}, \tag{7}$$

where ρ_{s} and ρ_{f} are the density of the solid and fluid components and **n** is the normal to the surfaces at which the fluid and solid components meet, κ_{f} is the bulk modulus of the fluid, $\boldsymbol{I}$ is the identity tensor and $\boldsymbol{c}$ is the isotropic tensor of elastic stiffnesses within the solid frame.

The fluid may be brine, hydrocarbon or a mix thereof, with the overall properties given in terms of the brine saturation S_{b} by

$$\rho_{\mathrm{f}} = S_{\mathrm{b}}\rho_{\mathrm{b}} + (1 - S_{\mathrm{b}})\rho_{\mathrm{h}}, \tag{8}$$

$$\frac{1}{\kappa_{\mathrm{f}}} = \frac{S_{\mathrm{b}}}{\kappa_{\mathrm{b}}} + \frac{1 - S_{\mathrm{b}}}{\kappa_{\mathrm{h}}} \tag{9}$$

and

$$\log\eta_{\mathrm{f}} = S_{\mathrm{b}}\log\eta_{\mathrm{b}} + (1 - S_{\mathrm{b}})\log\eta_{\mathrm{h}}, \tag{10}$$

where the subscripts b and h denote brine and hydrocarbon, respectively. The properties of brine as a function of temperature, pressure and salinity and those of hydrocarbons as a function of temperature, pressure and composition are discussed in Batzle & Wang (1992). The properties of the mixture become considerably more complex when we start to consider dissolved gas in either brine or oil phases, or other fluid interactions.

We shall assume then that the medium is macroscopically homogeneous and isothermal, and that the scaling of the solid and fluid properties is such that homogenization reduces the linearized compressible Navier–Stokes equations, elasticity equations and boundary conditions to the Biot equations. There is no definitive notation associated with the Biot equations so, using Boutin *et al.* (1987) and Schanz (2001), we write the equations of poroelasticity in terms of macroscopic variables as the constitutive relations

$$\boldsymbol{\tau} = \boldsymbol{c} : \boldsymbol{e} + \frac{\alpha}{\beta}\boldsymbol{I}(\alpha\nabla\cdot\mathbf{u} + \nabla\cdot\mathbf{w}) \tag{11}$$

and

$$\zeta = \alpha\nabla\cdot\mathbf{u} + \beta p, \tag{12}$$

the dynamic equations

$$\nabla\cdot\boldsymbol{\tau} = \rho\ddot{\mathbf{u}} + \rho_{\mathrm{f}}\ddot{\mathbf{w}} - \mathbf{F} \tag{13}$$

and

$$-\nabla p - \rho_{\mathrm{f}}\ddot{\mathbf{u}} = \tilde{Y}(\partial_t)\dot{\mathbf{w}} \tag{14}$$

and the mass balance equation

$$\dot{\zeta} + \nabla\cdot\dot{\mathbf{w}} = a(t), \tag{15}$$

where $\boldsymbol{\tau}(\mathbf{x})$, $\boldsymbol{e}(\mathbf{x})$ and $\mathbf{u}(\mathbf{x})$ now stand for the stress, strain and displacement in the solid averaged over a small region centred on **x**. **w** denotes the average fluid displacement relative to the solid, measured in volume per unit area so that

$$\mathbf{w} = \phi(\mathbf{U} - \mathbf{u}), \tag{16}$$

where **U** is the absolute fluid displacement, averaged as above, ϕ is the matrix porosity, ζ is the variation of fluid volume per unit reference volume and ρ is the average density of the saturated porous medium,

$$\rho = (1 - \phi)\rho_{\mathrm{s}} + \phi\rho_{\mathrm{f}}. \tag{17}$$

The Biot–Willis parameter α, the change in pore volume per unit change in bulk volume under drained conditions (Kümpel 1991), is given by

$$\alpha = 1 - \kappa/\kappa_{\mathrm{s}} \tag{18}$$

in terms of the bulk modulus of the frame κ, and that of the grain or mineral κ_s. From Kümpel (1991) α satisfies the bounds

$$\frac{3\phi(1-\nu_s)}{2(1-2\nu_s)+\phi(1+\nu_s)} \leq \alpha \leq 1, \tag{19}$$

where ν_s is the Poisson ratio of the solid component. The lower limit results from the Hashin–Shtrikman bound. The bulk moduli are defined as (Brown & Korringa 1975)

$$\kappa^{-1} = -\frac{1}{V}\frac{\partial V}{\partial p_d}\bigg|_p, \tag{20}$$

$$\kappa_s^{-1} = -\frac{1}{V}\frac{\partial V}{\partial p}\bigg|_{p_d} \tag{21}$$

and there is the additional bulk modulus

$$\kappa_\phi^{-1} = -\frac{1}{\phi V}\frac{\partial \phi V}{\partial p}\bigg|_{p_d}, \tag{22}$$

where the differential pressure p_d is given in terms of the external pressure p_e, by $p_d = p_e - p$. The parameter β is given by Brown & Korringa (1975) as

$$\beta = \frac{\alpha}{\kappa_s} + \phi\left(\frac{1}{\kappa_f} - \frac{1}{\kappa_\phi}\right), \tag{23}$$

and is related to the Skempton ratio B, the change in pore pressure per unit change in confining pressure under undrained conditions (Kümpel 1991), by

$$\beta = \frac{\alpha}{\kappa}(B^{-1} - \alpha). \tag{24}$$

Clearly, for a medium homogeneous and isotropic on the microscale, $\kappa_\phi = \kappa_s$, as assumed by Biot, and β reduces to

$$\beta = \frac{\alpha - \phi}{\kappa_s} + \frac{\phi}{\kappa_f}. \tag{25}$$

Even with these definitions of the various bulk moduli, there is a certain difficulty with their interpretation and measurement (Berryman 1981a,b; Korringa 1981), a detailed description of which is given by Kümpel (1991).

Finally, **F** is the bulk body force per unit volume, $a(t)$ is a fluid volume source term and $\bar{Y}(\partial_t)$ is the viscodynamic operator (Biot 1962a,b). Below the Biot characteristic frequency

$$\omega_c = \eta_f \phi / K \rho_f \tag{26}$$

Poiseuille flow holds and

$$\bar{Y}(\partial_t) = \eta_f / K + q\,\partial_t, \tag{27}$$

where K is the permeability and $q = m\rho_f/\phi$ with m being the tortuosity coefficient (Johnson *et al.* 1982) dependent upon the pore geometry.

Above the critical frequency ω_c, η_f must be replaced by a modified complex viscosity

$$\bar{\eta}_f = \eta_f F(\omega d/\omega_c), \tag{28}$$

where d is a coefficient that depends on the geometry of the pores and the function F is given by Biot (1956). However, homogenization is only possible at low Reynolds number (Auriault 1991) so we may readily assume that eq. (27) holds.

Assuming an implicit $e^{-i\omega t}$ dependence, or equivalently Fourier transforming all variables and assuming vanishing initial conditions, eqs (13)–(15) become

$$\nabla \cdot \boldsymbol{\tau} = -\omega^2(\rho \mathbf{u} + \rho_f \mathbf{w}) - \mathbf{F}, \tag{29}$$

$$-\nabla p + \rho_f \omega^2 \mathbf{u} = -\left(q\omega^2 + i\omega\eta_f/K\right)\mathbf{w} \tag{30}$$

and

$$\zeta + \nabla \cdot \mathbf{w} = V, \tag{31}$$

where

$$V = \int_0^t a(t')\,dt' \tag{32}$$

is the volume of injected fluid due to the source $a(t)$.

While there are many parameters involved in the description of a Biot medium, they are not all independent, and the use of empirical relations derived from well log and laboratory data may be used to constrain a number of the parameters. The Biot–Willis parameter α (eq. 18) is largely a function of porosity ϕ in sandstones (e.g. Murphy *et al.* 1993), though the form of the relation is also dependent upon the porosities at which the material transitions between a suspension and an unconsolidated grain-supported phase ϕ_0, between an unconsolidated and a

consolidated grain-supported phase ϕ_c, and (weakly) on the clay content (Vernik 1998); we choose to follow Vernik (1998) in defining α in terms of ϕ as

$$\alpha = \begin{cases} A\phi - B\phi^2 & \phi \le \phi_c \\ 1 - C(\phi_0 - \phi) + D\left(\phi_0^2 - \phi^2\right) & \phi_c < \phi < \phi_0 \\ 1 & \phi \ge \phi_0 \end{cases} \tag{33}$$

for a given set of constants dependent on the properties of the matrix and the clay content. It is the middle, unconsolidated phase, where the relationship is most uncertain, dependent upon the competing processes of cementation and compaction during the early diagenetic history of the sediment.

We may define a parameter ς, similarly dependent on porosity and clay content to α,

$$\varsigma = 1 - \mu/\mu_s \tag{34}$$

that constrains the shear modulus of the frame in terms of that of the mineral.

There have been many attempts to correlate permeability and porosity as a means of estimating the former in terms of the latter in well log data. The difficulty that this idea encounters is based on the principle that porosity is a function of grain sorting while permeability is a direct function of grain size, so that any relation between them becomes a function of the pore geometry. Empirical relations, often referred to as Kozeny–Carman relations, are frequently used. We choose to adopt a version that additionally includes such scalefactors as the tortuosity (Prasad 2003)

$$K = \frac{1}{F_s m^2 S_{Vgr}^2} \frac{\phi^3}{(1-\phi)^2}, \tag{35}$$

with K being measured in μm^2, where 1 $D = 0.986\,923\ \mu m^2$. F_s is a pore shape parameter and S_{Vgr} is the specific surface area per unit grain volume, both of which are difficult to measure. However, Prasad (2003) argues that the combined term $1/F_s m^2 S_{Vgr}^2$, the square root of which she calls the 'flow zone indicator', may be estimated via correlations within individual geological units.

The experiments of Johnson *et al.* (1982) suggest a relation of the form

$$m = \phi^{-a}, \quad 0 \le a \le 1, \tag{36}$$

for the tortuosity, with $a = 0.5$ for their experiments involving fused-glass-bead samples, though, in all likelihood this is overly simplified and takes a more complex form in natural rock.

3 THE EQUATIONS OF PROPAGATION

Setting $\mathbf{F}$ and V to zero, $\boldsymbol{\tau}$, p and ζ are eliminated from eqs (11), (12), (29)–(31) to deduce that

$$\mu\nabla^2\mathbf{u} + (\lambda+\mu)\nabla(\nabla\cdot\mathbf{u}) = -\omega^2(\rho - \alpha\rho_f)\mathbf{u} - \left[\rho_f\omega^2 - \alpha\left(q\omega^2 + i\omega\eta_f/K\right)\right]\mathbf{w} \tag{37}$$

and

$$\frac{1}{\beta}\nabla[\nabla\cdot(\alpha\mathbf{u} + \mathbf{w})] = -\rho_f\omega^2\mathbf{u} - \left(q\omega^2 + i\omega\eta_f/K\right)\mathbf{w}. \tag{38}$$

By Helmholtz' theorem, we write

$$\mathbf{u} = \nabla\Phi_u + \nabla\wedge\boldsymbol{\Psi}_u \tag{39}$$

and

$$\mathbf{w} = \nabla\Phi_w + \nabla\wedge\boldsymbol{\Psi}_w, \tag{40}$$

where $\nabla\cdot\boldsymbol{\Psi}_u = 0$ and $\nabla\cdot\boldsymbol{\Psi}_w = 0$, and it may be deduced that

$$\{\mu\nabla^2 + \mathring{\rho}\omega^2\}\boldsymbol{\Psi}_u = 0 \tag{41}$$

and

$$\left\{(\lambda+2\mu)\nabla^4 + \left[\mathring{\rho}\omega^2 - \frac{(\lambda+2\mu)\beta + \mathring{\alpha}^2}{\theta}\right]\nabla^2 - \frac{\beta\mathring{\rho}\omega^2}{\theta}\right\}\Phi_u = 0, \tag{42}$$

and that

$$\boldsymbol{\Psi}_w = \rho_f\omega^2\theta\boldsymbol{\Psi}_u \tag{43}$$

and

$$\Phi_w = -\frac{\theta}{\mathring{\alpha}}\left[\omega^2(\mathring{\rho} - \mathring{\alpha}\rho_f)\Phi_u + (\lambda+2\mu)\nabla^2\Phi_u\right], \tag{44}$$

where the notation

$$\mathring{\rho} = \rho + \rho_f^2\omega^2\theta, \tag{45}$$

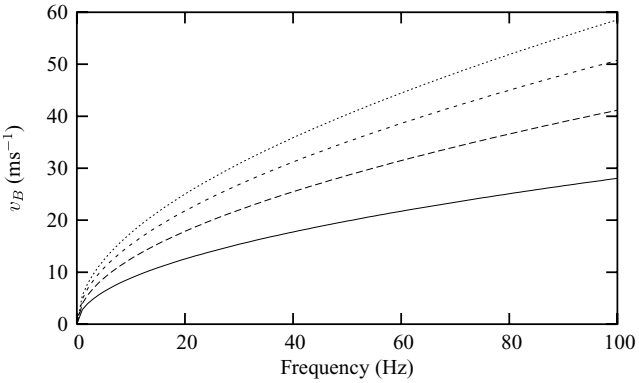

Figure 1. Variation in wave speed of the slow compressional wave with frequency for the uncracked case (solid line) and crack volume densities of 0.001 (long dashes), 0.002 (short dashes) and 0.003 (dotted line) at vertical incidence.

$$\mathring{\alpha} = \alpha + \rho_{\rm f}\omega^2\theta \tag{46}$$

and

$$\theta = -\left(q\omega^2 + {\rm i}\omega\eta_{\rm f}/K\right)^{-1} \tag{47}$$

has been used.

Rewriting eqs (41) and (42) as

$$\left(\nabla^2 + k_3^2\right)\boldsymbol{\Psi}_u = 0 \tag{48}$$

and

$$\left(\nabla^2 + k_1^2\right)\left(\nabla^2 + k_2^2\right)\Phi_u = 0 \tag{49}$$

determines the one shear and two compressional wavenumbers. There are, in fact, two shear waves, with different polarity, as there are two degrees of freedom in the definition of $\boldsymbol{\Psi}_u$. Clearly, then,

$$\mathbf{u} = \nabla\Phi_1 + \nabla\Phi_2 + \nabla \wedge \boldsymbol{\Psi} \tag{50}$$

and

$$\mathbf{w} = \chi_1\nabla\Phi_1 + \chi_2\nabla\Phi_2 + \chi_3\nabla \wedge \boldsymbol{\Psi}, \tag{51}$$

where $\nabla \cdot \boldsymbol{\Psi} = 0$,

$$\chi_i = \frac{\theta k_i^2}{\mathring{\alpha}}\left[(\lambda + 2\mu) - v_i^2(\mathring{\rho} - \mathring{\alpha}\rho_{\rm f})\right], \quad i = 1, 2 \tag{52}$$

$$\chi_3 = \rho_{\rm f}\omega^2\theta \tag{53}$$

and $v_i = \omega/k_i$ are the wave speeds. Hence

$$p = C_1k_1^2\Phi_1 + C_2k_2^2\Phi_2, \tag{54}$$

where

$$C_i = \frac{1}{\mathring{\alpha}}\left(\mathring{\rho}v_i^2 - \lambda - 2\mu\right), \quad i = 1, 2. \tag{55}$$

As a numerical example, we consider a brine-saturated sandstone with the following parameter values for the matrix: $\rho_{\rm s} = 2.65 \times 10^3$ kg m^{-3}, $\kappa_{\rm s} = 35.7$ GPa and $\mu_{\rm s} = 33.0$ GPa. Taking $\phi = 0.2$, we assume $K = 0.1$ μm^2, $m = 2.0$, $\alpha = 0.597$ and $\varsigma = 0.576$. The brine has parameters $\rho_{\rm f} = 1.09 \times 10^3$ kg m^{-3}, $\kappa_{\rm f} = 3.26$ GPa and $\eta_{\rm f} = 0.48 \times 10^{-3}$ Pa s, at a temperature of 65 °C, pressure of 25 MPa and 150 000 ppm NaCl (Batzle & Wang 1992).

Fig. 1 shows the variation with frequency of the wave speed of the slow compressional (Biot) wave (the solid line) over the seismic bandwidth. There is a considerable increase in the wave speed with frequency from the static limit where the wave is absent, however, it remains well below the speed of waves that are likely to be observed in seismic reflection data, furthermore it has highly attenuative behaviour.

The fast compressional and shear waves show negligible changes in wave speed or attenuation with frequency over the seismic range; it is not until approaching the characteristic frequency (eq. 26) at around 0.9 MHz that a significant change is seen in these wave speeds.

4 DETERMINING GREEN'S FUNCTIONS

Using the method of smoothing will require a representation of the scattered field within an inclusion in terms of an incident field. This is best achieved via the appropriate Green's function. To determine Green's functions, rather than taking the incomplete methods of Burridge &

Vargas (1979) and Norris (1985), we follow Boutin *et al.* (1987), where the response of the system to an impulsive forcing term at a point **y** is required. Into eqs (29) and (31) we introduce Dirac delta functions:

$$\nabla \cdot \boldsymbol{\tau} = -\omega^2(\rho \mathbf{u} + \rho_f \mathbf{w}) - \mathbf{F}\delta(\mathbf{x} - \mathbf{y}) \tag{56}$$

and

$$\zeta + \nabla \cdot \mathbf{w} = V\delta(\mathbf{x} - \mathbf{y}). \tag{57}$$

Given the relation between **u** and **w** (eqs 50 and 51), eqs (11), (12), (30), (56) and (57) may be reduced to a set of four equations by eliminating $\boldsymbol{\tau}$, **w** and ζ to yield

$$\mu\nabla^2\mathbf{u} + (\lambda + \mu)\nabla(\nabla \cdot \mathbf{u}) + \mathring{\rho}\omega^2\mathbf{u} - \mathring{\alpha}\nabla p = -\mathbf{F}\delta(\mathbf{x} - \mathbf{y}) \tag{58}$$

and

$$\theta\nabla^2 p - \beta p - \mathring{\alpha}\nabla \cdot \mathbf{u} = -V\delta(\mathbf{x} - \mathbf{y}). \tag{59}$$

Eqs (58) and (59) may be written as

$$\boldsymbol{\mathcal{L}}\mathbf{R} = -\boldsymbol{S}\delta(\mathbf{x} - \mathbf{y}), \tag{60}$$

where the source and response four-vectors are defined as

$$\boldsymbol{S} = \begin{pmatrix} \mathbf{F} \\ V \end{pmatrix} \tag{61}$$

and

$$\mathbf{R} = \begin{pmatrix} \mathbf{u} \\ p \end{pmatrix} \tag{62}$$

and the components of the operator $\boldsymbol{\mathcal{L}}$ are given by

$$\mathcal{L}_{ij} = \begin{pmatrix} c_{ipjq}\partial_p\partial_q + \mathring{\rho}\omega^2\delta_{ij} & -\mathring{\alpha}\partial_i \\ -\mathring{\alpha}\partial_j & \theta\nabla^2 - \beta \end{pmatrix}. \tag{63}$$

$\boldsymbol{\mathcal{L}}$ is a 4-D second-rank tensor and the notation that we have adopted here is such that the upper left-hand coefficient represents the 3-D minor $\{\mathcal{L}_{ij} : 1 \le i, j \le 3\}$, the lower right-hand term corresponds to $\mathcal{L}_{44}$ and the upper right- and lower left-hand coefficients represent $\{\mathcal{L}_{i4} : 1 \le i \le 3\}$ and $\{\mathcal{L}_{4j} : 1 \le j \le 3\}$, respectively. The Green functions then solve

$$\boldsymbol{\mathcal{L}}\mathbf{G}(\mathbf{x}, \mathbf{y}) = -\boldsymbol{I}\delta(\mathbf{x} - \mathbf{y}). \tag{64}$$

This method has yielded a set of four equations, rather than the six given by some authors (e.g. Sahay 2001), and further have the advantage that the operator $\boldsymbol{\mathcal{L}}$ is symmetric.

The method used by Boutin *et al.* (1987) to solve for **G** is that of Kupradze (1979). A similar method is used by Sahay (2001) for a 6×6, rather than a 4×4 system. Letting $\boldsymbol{\mathcal{L}}^\dagger$ be the differential operator corresponding to the cofactors of $\boldsymbol{\mathcal{L}}$, then if the scalar function ϕ solves

$$\det \boldsymbol{\mathcal{L}}\phi = -\delta(\mathbf{x} - \mathbf{y}), \tag{65}$$

Green's functions are given by

$$\mathbf{G} = \boldsymbol{\mathcal{L}}^\dagger\phi. \tag{66}$$

In particular,

$$\boldsymbol{\mathcal{L}}^\dagger = \boldsymbol{\mathcal{L}}^\ddagger\mu\left(\nabla^2 + k_3^2\right) \tag{67}$$

and

$$\det \boldsymbol{\mathcal{L}} = \mu\left(\nabla^2 + k_3^2\right)D, \tag{68}$$

so that if ψ solves

$$D\psi = -\delta(\mathbf{x} - \mathbf{y}), \tag{69}$$

$$\mathbf{G} = \boldsymbol{\mathcal{L}}^\ddagger\psi, \tag{70}$$

where

$$D = \mu(\lambda + 2\mu)\theta\left(\nabla^2 + k_1^2\right)\left(\nabla^2 + k_2^2\right)\left(\nabla^2 + k_3^2\right) \tag{71}$$

and $\boldsymbol{\mathcal{L}}^\ddagger$ is given by comparison with Boutin *et al.* (1987).

This leads to

$$4\pi G_{ij}(\mathbf{x},\mathbf{y}) = \begin{pmatrix} -\partial_i\partial_j \sum_{p=1}^{3} \alpha_p \frac{e^{ik_p r}}{r} + \frac{\delta_{ij}}{\mu}\frac{e^{ik_3 r}}{r} & -\partial_i \sum_{p=1}^{2} \xi(-1)^p \frac{e^{ik_p r}}{r} \\ -\partial_j \sum_{p=1}^{2} \xi(-1)^p \frac{e^{ik_p r}}{r} & -\frac{1}{\theta\alpha_3}\left(\alpha_2 \frac{e^{ik_1 r}}{r} + \alpha_1 \frac{e^{ik_2 r}}{r}\right) \end{pmatrix}, \tag{72}$$

where

$$\alpha_1 = \frac{k_2^2 - \mu k_3^2/(\lambda+2\mu)}{\mu k_3^2\left(k_2^2 - k_1^2\right)}, \tag{73}$$

$$\alpha_2 = \frac{k_1^2 - \mu k_3^2/(\lambda+2\mu)}{\mu k_3^2\left(k_1^2 - k_2^2\right)}, \tag{74}$$

$$\alpha_3 = \frac{-1}{\mu k_3^2}, \tag{75}$$

$$\xi = \frac{1}{\chi_1 - \chi_2} \tag{76}$$

and $r = |\mathbf{x} - \mathbf{y}|$.

Green's functions have the symmetry

$$G_{ij}(\mathbf{x},\mathbf{y}) = G^*_{ji}(\mathbf{y},\mathbf{x}), \tag{77}$$

where $\mathbf{G}^*$ is the adjoint function to $\mathbf{G}$ and solves the problem

$$\boldsymbol{\mathcal{L}}^*\mathbf{G}^*(\mathbf{x},\mathbf{y}) = -\boldsymbol{I}\delta(\mathbf{x}-\mathbf{y}), \tag{78}$$

with $\boldsymbol{\mathcal{L}}^*$ the operator adjoint to $\boldsymbol{\mathcal{L}}$.

The operator $\boldsymbol{\mathcal{L}}$ may be written as

$$\boldsymbol{\mathcal{L}} = \boldsymbol{\mathcal{L}}^0 + \boldsymbol{\mathcal{L}}^{\mathrm{p}}, \tag{79}$$

where

$$\mathcal{L}^0_{ij} = \begin{pmatrix} c^s_{ipjq}\partial_p\partial_q + \rho_{\mathrm{s}}\omega^2\delta_{ij} & 0 \\ 0 & 0 \end{pmatrix} \tag{80}$$

represents the purely elastic contribution, with $\boldsymbol{c}^{\mathrm{s}}$ the isotropic elastic stiffness tensor of the mineral, with shear modulus μ_{s} and bulk modulus κ_{s}, and the remaining terms are bundled into

$$\mathcal{L}^{\mathrm{p}}_{ij} = \begin{pmatrix} -c^p_{ipjq}\partial_p\partial_q + \left[\phi(\rho_{\mathrm{f}} - \rho_{\mathrm{s}}) + \rho_{\mathrm{f}}^2\omega^2\theta\right]\omega^2\delta_{ij} & -\left[\alpha + \rho_{\mathrm{f}}\omega^2\theta\right]\partial_i \\ -\left[\alpha + \rho_{\mathrm{f}}\omega^2\theta\right]\partial_j & \theta\nabla^2 - \beta \end{pmatrix}, \tag{81}$$

which represents the contribution from the pores, where the isotropic tensor $\boldsymbol{c}^{\mathrm{p}}$ is given in terms of the scaled shear and bulk moduli $\varsigma\mu_{\mathrm{s}}$ and $\alpha\kappa_{\mathrm{s}}$.

As porosity $\phi \to 0$, $\theta \to 0$ and, from empirical relations $\alpha \to 0$ and $\varsigma \to 0$, thus $\beta \to 0$ so that the dynamic equations for the fluid and solid decouple with the fluid terms vanishing identically; the poroelastic theory reduces to an elastic one.

The limit in which the porosity $\phi \to 1$ is a little more complex. Experiments suggests that $\alpha \to 1$ and $\varsigma \to 1$ (Murphy *et al.* 1993; Vernik 1998), so that $\boldsymbol{c}^{\mathrm{p}}$ directly cancels with $\boldsymbol{c}^{\mathrm{s}}$. Furthermore, $\rho_{\mathrm{f}}\omega^2\theta \to -1$ on the proviso that $m \to 1$, as indicated by Johnson *et al.* (1982) (eq. 36) and $K \to \infty$, as predicted by a number of commonly used Kozeny–Carman relations (e.g. eq. 35). At this point the solid and fluid equations have once again decoupled, with the solid terms vanishing identically and the fluid terms leaving a wave equation for the pressure in the fluid.

5 THE METHOD OF SMOOTHING

Hudson (1980) uses the method of smoothing (Keller 1964) to determine the overall properties of an elastic medium containing cracks. By direct analogy with his method, we now derive the corresponding results for a poroelastic medium. If we let a be a characteristic length-scale associated with the cracks, and it is assumed that $l \ll a \ll L$, and that the porous matrix remains homogeneous on both the micro and macro scales, l and L, respectively, then the equations of poroelasticity may be used to describe the background matrix and the contents of the cracks that will be inserted into the matrix.

Let $\mathbf{R}^0(\mathbf{x})$ represent the incident, or unperturbed wave, such that

$$\boldsymbol{\mathcal{L}}\mathbf{R}^0(\mathbf{x}) = 0, \quad \mathbf{x} \in \mathcal{D}, \tag{82}$$

where $\mathcal{D}$ is a region of the poroelastic material containing no cracks. If we introduce cracks embedded within $\mathcal{D}$ then we seek the solution of

$$\boldsymbol{\mathcal{L}}\mathbf{R}(\mathbf{x}) = 0, \quad \mathbf{x} \in \mathcal{D}', \tag{83}$$

where $\mathcal{D}'$ is the part of $\mathcal{D}$ outside the cracks.

If $\epsilon \boldsymbol{S}^n$ is the scattering operator associated with the nth crack, so that $\epsilon \boldsymbol{S}^n \mathbf{R}^n(\mathbf{x})$ is the scattered wave due to the wave $\mathbf{R}^n(\mathbf{x})$ incident on the crack and the small scalar ϵ indicates that the scattered field is small, in some manner, then

$$\mathbf{R}^n(\mathbf{x}) + \epsilon \boldsymbol{S}^n \mathbf{R}^n(\mathbf{x}) = \mathbf{R}(\mathbf{x}). \tag{84}$$

Similarly, if there are N cracks,

$$\mathbf{R}(\mathbf{x}) = \mathbf{R}^0(\mathbf{x}) + \epsilon \sum_{n=1}^{N} \boldsymbol{S}^n \mathbf{R}^n(\mathbf{x}), \quad \mathbf{x} \in \mathcal{D}', \tag{85}$$

so that

$$\mathbf{R}^n(\mathbf{x}) = \mathbf{R}^0(\mathbf{x}) + \epsilon \sum_{n \neq m} \boldsymbol{S}^n \mathbf{R}^n(\mathbf{x}), \quad \mathbf{x} \in \mathcal{D}'_n, \tag{86}$$

where $\mathcal{D}'_n$ is the region of $\mathcal{D}$ excluding all but the nth crack. Successive approximations lead to

$$\mathbf{R}(\mathbf{x}) = \mathbf{R}^0(\mathbf{x}) + \epsilon \sum_{n=1}^{N} \boldsymbol{S}^n \mathbf{R}^0(\mathbf{x}) + \mathcal{O}(\epsilon^2), \quad \mathbf{x} \in \mathcal{D}'. \tag{87}$$

Considering the distribution of cracks as a statistical ensemble, we take the average of eq. (87) and assume that the statistical properties of each crack are the same, such that

$$\langle \mathbf{R} \rangle(\mathbf{x}) = \{1 + \epsilon N \langle \boldsymbol{S} \rangle(\mathbf{x}) + \mathcal{O}(\epsilon^2)\} \mathbf{R}^0(\mathbf{x}), \tag{88}$$

where the operator $\langle \cdot \rangle$ indicates the average.

Assuming that all the cracks are of the same size, orientation and infill, and that the statistical distribution of each crack is homogeneous, we may write

$$N \langle \boldsymbol{S} \rangle(\mathbf{x}) = \nu^{\mathrm{s}} \int_{\mathcal{D}} dV_\xi \; \bar{\boldsymbol{S}}(\mathbf{x}, \boldsymbol{\xi}), \tag{89}$$

where $\nu^{\mathrm{s}} = N/V$ is the number density of cracks and $\boldsymbol{\xi}$ is the position of the centroid of a crack. Then, inverting eq. (88) for $\mathbf{R}^0(\mathbf{x})$ and applying $\boldsymbol{\mathcal{L}}$ to the result yields

$$\left[\boldsymbol{\mathcal{L}} - \epsilon \nu^{\mathrm{s}} \int_{\mathcal{D}} dV_\xi \; \boldsymbol{\mathcal{L}} \bar{\boldsymbol{S}}(\mathbf{x}, \boldsymbol{\xi}) + \mathcal{O}(\epsilon^2) \right] \langle \mathbf{R} \rangle(\mathbf{x}) = 0. \tag{90}$$

We write the mean wave as

$$\langle \mathbf{R} \rangle(\mathbf{x}) = \mathbf{b} \mathrm{e}^{\mathrm{i}\mathbf{k}\cdot\mathbf{x}} \tag{91}$$

for some vectors $\mathbf{b}$ and $\mathbf{k}$, where $\mathbf{b}$ is a four-vector.

The zeroth-order solution, corresponding to $\epsilon = 0$, is given by eq. (83). From eq. (68) this leads to the dispersion equation

$$\mu^2(\lambda + 2\mu)\theta \left(k_1^2 - k^2\right)\left(k_2^2 - k^2\right)\left(k_3^2 - k^2\right)^2 = 0, \tag{92}$$

which clearly has four solutions satisfying the radiation condition, corresponding to two shear waves with wave speed ω/k_3 and compressional waves with wave speeds ω/k_1 and ω/k_2.

6 THE SCATTERED WAVE

If the average crack occupies the region V', then the complete field is given by

$$\mathbf{R}(\mathbf{x}) = \begin{cases} \langle \mathbf{R} \rangle + \mathbf{R}^{\mathrm{s}} & \mathbf{x} \notin V' \\ \langle \mathbf{R} \rangle + \mathbf{R}' & \mathbf{x} \in V', \end{cases} \tag{93}$$

such that the scattered wave is given by

$$\epsilon \bar{\boldsymbol{S}} \langle \mathbf{R} \rangle(\mathbf{x}) = \begin{cases} \mathbf{R}^{\mathrm{s}} & \mathbf{x} \notin V' \\ \mathbf{R}' & \mathbf{x} \in V'. \end{cases} \tag{94}$$

Boundary integral equations for the poroelastic problem are derived by Manolis & Beskos (1989) and Schanz (2001). We follow Schanz (2001) in writing

$$\int_{\mathcal{D} \setminus V'} \left[\boldsymbol{\mathcal{L}}_{\mathbf{y}} \mathbf{R}^{\mathrm{s}}(\mathbf{y}) \mathbf{G}^*(\mathbf{y}, \mathbf{x}) - \mathbf{R}^{\mathrm{s}}(\mathbf{y}) \boldsymbol{\mathcal{L}}^*_{\mathbf{y}} \mathbf{G}^*(\mathbf{y}, \mathbf{x}) \right] dV_{\mathbf{y}} = \int_{\partial V'_+} \left[\mathbf{R}^{\mathrm{s}}(\mathbf{y}) \mathbf{T}^*(\mathbf{y}, \mathbf{x}) - \mathbf{V}^{\mathrm{s}}(\mathbf{y}) \mathbf{G}^*(\mathbf{y}, \mathbf{x}) \right] dS_{\mathbf{y}}, \tag{95}$$

where

$$V_i^s = \tau_{ij}^s n_j = \left(c_{ijpq} u_{p,q}^s - \delta_{ij} \alpha p^{\mathrm{s}} \right) n_j \tag{96}$$

and

$$V_4^s = -w_j^s n_j = -\theta \left(-p^{\mathrm{s}}_{,j} + \rho_{\mathrm{f}}\omega^2 u_j^s\right) n_j \tag{97}$$

are the traction and normal flux, respectively, and we define the 'adjoint' terms

$$T^*_{i\gamma} = (c_{ijpq} G^*_{p\gamma,q} + \delta_{ij}\alpha G^*_{4\gamma}) n_j \tag{98}$$

and

$$T^*_{4\gamma} = -\theta \left(-G^*_{4\gamma,j} - \rho_{\mathrm{f}}\omega^2 G^*_{j\gamma}\right) n_j, \tag{99}$$

where the index γ ranges from 1 to 4 while the others only go as far as 3 and $\mathbf{n}$, the normal to the surface $\partial V'_+$, points out of the volume V'. The subscript + on $\partial V'$ indicates that the integral is constructed from limiting values as the boundary is approached from outside and the subscript $\mathbf{y}$ on $\boldsymbol{\mathcal{L}}$ and $\boldsymbol{\mathcal{L}}^*$ indicate the variable with respect to which differentiation is assumed.

Now,

$$\boldsymbol{\mathcal{L}}_{\mathbf{y}} \mathbf{R}^{\mathrm{s}}(\mathbf{y}) = 0, \quad \mathbf{y} \notin V' \tag{100}$$

and

$$\boldsymbol{\mathcal{L}}^*_{\mathbf{y}} \mathbf{G}^*(\mathbf{y}, \mathbf{x}) = -\boldsymbol{I}\delta(\mathbf{y} - \mathbf{x}), \quad \mathbf{y} \notin V' \tag{101}$$

then

$$\int_{\partial V'_+} [\mathbf{R}^{\mathrm{s}}(\mathbf{y})\mathbf{T}^*(\mathbf{y}, \mathbf{x}) - \mathbf{V}^{\mathrm{s}}(\mathbf{y})\mathbf{G}^*(\mathbf{y}, \mathbf{x})]\, dS_{\mathbf{y}} = \begin{cases} \mathbf{R}^{\mathrm{s}}(\mathbf{x}) & \mathbf{x} \notin V' \\ 0 & \mathbf{x} \in V'. \end{cases} \tag{102}$$

Similarly, inside the inclusion, we may write

$$\int_{V'} \left\{\boldsymbol{\mathcal{L}}'_{\mathbf{y}}[\mathbf{R}^0(\mathbf{y}) + \mathbf{R}'(\mathbf{y})]\mathbf{G}^*(\mathbf{y}, \mathbf{x}) - \mathbf{R}'(\mathbf{y})\boldsymbol{\mathcal{L}}^*_{\mathbf{y}}\mathbf{G}^*(\mathbf{y}, \mathbf{x})\right\} dV_{\mathbf{y}} = \begin{cases} 0 & \mathbf{x} \notin V' \\ \mathbf{R}'(\mathbf{x}) & \mathbf{x} \in V', \end{cases} \tag{103}$$

where $\boldsymbol{\mathcal{L}}'$ is the same operator as $\boldsymbol{\mathcal{L}}$ but with material parameters (also marked with a prime) corresponding to the porous medium of the inclusion, so that

$$\boldsymbol{\mathcal{L}}'_{\mathbf{y}}[\mathbf{R}^0(\mathbf{y}) + \mathbf{R}'(\mathbf{y})] = 0 \quad \mathbf{y} \in V'. \tag{104}$$

All of the material parameters of the porous medium of the inclusion may differ from those of the matrix apart from the properties of the fluid. So that an open-pore boundary condition may be assumed between the two porous media, with the fluid pressure continuous across the boundary, the restriction that the two materials are saturated with the same fluid is imposed.

Expanding the left-hand side of eq. (103) and adding eq. (102) yields an expression for the scattered wave (eq. 94)

$$\epsilon \bar{S}_{kj} \langle R_j \rangle(\mathbf{x}; \boldsymbol{\xi}) = \int_{V'} \left[G_{ki}(\mathbf{x}, \mathbf{y})\mathcal{A}_{ip} + \frac{\partial G_{ki}(\mathbf{x}, \mathbf{y})}{\partial x_j}\mathcal{B}_{ijp} \right] R_p(\mathbf{y}; \boldsymbol{\xi})\, d\mathrm{V}_{\mathbf{y}}, \tag{105}$$

where the operators $\boldsymbol{\mathcal{A}}$ and $\boldsymbol{\mathcal{B}}$ are given by

$$\mathcal{A}_{ip} = \begin{pmatrix} \hat{\rho}^+\omega^2\delta_{ip} & -\rho_{\mathrm{f}}\omega^2\theta^+\partial_i \\ -\alpha^+\partial_p & -\beta^+ \end{pmatrix} \tag{106}$$

and

$$\mathcal{B}_{ijp} = \begin{pmatrix} c^+_{ijpq}\partial_q & -\alpha^+\delta_{ij} \\ -\rho_{\mathrm{f}}\omega^2\theta^+\delta_{jp} & \theta^+\partial_j \end{pmatrix} \tag{107}$$

and act on the variable $\mathbf{y}$, where we have applied the boundary conditions between two porous media with wholly connected pore spaces (Deresiewicz & Skalak 1963; Altay & Dökmeci 1998); continuity of solid displacement

$$u_i^s = u'_i, \tag{108}$$

continuity of fluid pressure

$$p^{\mathrm{s}} = p', \tag{109}$$

continuity of traction

$$\left[c_{ijpq}\left(u^0_{p,q} + u^s_{p,q}\right) - \delta_{ij}\alpha(p^0 + p^{\mathrm{s}})\right] n_j = \left[c'_{ijpq}\left(u^0_{p,q} + u'_{p,q}\right) - \delta_{ij}\alpha'(p^0 + p')\right] n_j \tag{110}$$

and continuity of normal flux

$$\theta\left[-\left(p^0_{,j} + p^s_{,j}\right) + \rho_{\mathrm{f}}\omega^2\left(u^0_j + u^s_j\right)\right] n_j = \theta'\left[-\left(p^0_{,j} + p'_{,j}\right) + \rho_{\mathrm{f}}\omega^2\left(u^0_j + u'_j\right)\right] n_j. \tag{111}$$

Furthermore, we have defined the total field within V' as

$$\begin{pmatrix} \mathbf{u} \\ p \end{pmatrix} = \begin{pmatrix} \mathbf{u}^0 \\ p^0 \end{pmatrix} + \begin{pmatrix} \mathbf{u}' \\ p' \end{pmatrix} \tag{112}$$

and

$$\boldsymbol{c}^{+} = \boldsymbol{c}' - \boldsymbol{c}, \tag{113}$$

with θ^{+}, α^{+}, β^{+} and $\mathring{\rho}^{+}$ defined similarly. Finally, we have also made use of the reciprocity relation (eq. 77) and made explicit the dependence on the wavefield inside an inclusion on the location of the centroid $\boldsymbol{\xi}$ of the inclusion.

Substituting eq. (105) into the first-order term of eq. (90) gives

$$-\epsilon \int_{\mathcal{D}} \mathcal{L}_{ik} \bar{S}_{kj}(\mathbf{x};\boldsymbol{\xi}) \langle R_j \rangle(\mathbf{x})\, dV_{\xi} = \int_{V'} \left\{ [\mathcal{A}_{ip} R_p(\boldsymbol{\xi}+\mathbf{X};\boldsymbol{\xi})]\Big|_{\xi=\mathbf{x}-\mathbf{X}} + \frac{\partial}{\partial x_j}[\mathcal{B}_{ijp} R_p(\boldsymbol{\xi}+\mathbf{X};\boldsymbol{\xi})]\Big|_{\xi=\mathbf{x}-\mathbf{X}} \right\} dV_{\mathbf{X}}, \tag{114}$$

where we replaced $\mathbf{y}$ by $\boldsymbol{\xi}+\mathbf{X}$ in eq. (105) and used $\mathbf{X}$ as the variable of integration, so that all the derivatives in the operators $\boldsymbol{\mathcal{A}}$ and $\boldsymbol{\mathcal{B}}$ are with respect to $\mathbf{X}$.

7 THE EFFECTIVE MEDIUM

For the elastic problem the wavefield within the inclusion is approximated by Hudson (1994) using the static result of Eshelby (1957), greatly simplifying the corresponding expression to eq. (114). We use the same method in the poroelastic problem, using the result of Berryman (1997) for low (non-zero) frequencies. The fluid pressure within the inclusion is the same as that in the matrix (i.e. that due to the incident field) and therefore so is the pressure gradient. The solid displacement within the inclusion may be approximated by that due to the incident field, as with the elastic case (Kuster & Toksöz 1974; Hudson 1994; Tod 2003), again provided the frequencies are moderate, by making what is essentially a Born approximation. The strain in the inclusion $\boldsymbol{e}$ is related to the strain $\boldsymbol{e}^0$ and pressure p^0 due to the incident field by (Berryman 1997)

$$\boldsymbol{e} = \mathbf{E}\left(\boldsymbol{e}^0 - \frac{\alpha^{+}}{3\kappa^{+}} p^0 \boldsymbol{I}\right) + \frac{\alpha^{+}}{3\kappa^{+}} p^0 \boldsymbol{I}, \tag{115}$$

where κ^{+} is defined as the difference between the frame bulk moduli of the inclusion and matrix, similarly to all quantities with a $+$ superscript. $\mathbf{E}$ is given by

$$\mathbf{E} = (\boldsymbol{S}\mathbf{s}^0 \boldsymbol{c}^{+} + \boldsymbol{I})^{-1}, \tag{116}$$

in terms of the Eshelby tensor $\boldsymbol{S}$ and the frame bulk and shear moduli of the matrix and inclusion.

Provided we make the assumption that the inclusion can be described by an ellipsoid then the tensor $\mathbf{E}$ is uniform throughout the inclusion so that the integrand in eq. (114) is independent of the variable of integration $\mathbf{X}$. Thus, the volume integral in eq. (114) yields only a multiplicative constant s equal to the volume density of the inclusions

$$s = \frac{4}{3}\pi \nu^{s} abc \tag{117}$$

and we may write eq. (90) as

$$\mathcal{L}^{*}_{ip} \begin{pmatrix} u_p \\ p \end{pmatrix} = \begin{pmatrix} c^{*}_{ijpq}\partial_j\partial_q + \mathring{\rho}^{*}\omega^2\delta_{ip} & -\mathring{\alpha}^{*}_{ij}\partial_j \\ -\mathring{\alpha}^{*}_{pj}\partial_j & \theta^{*}\nabla^2 - \beta^{*} \end{pmatrix} \begin{pmatrix} u_p \\ p \end{pmatrix} = 0, \tag{118}$$

where

$$\mathring{\rho}^{*} = \rho^{*} + \rho_{\mathrm{f}}^2 \omega^2 \theta^{*}, \tag{119}$$

$$\mathring{\alpha}^{*}_{ij} = \alpha^{*}_{ij} + \rho_{\mathrm{f}}\omega^2\theta^{*}\delta_{ij} \tag{120}$$

and

$$\theta^{*} = \theta + s\theta^{+}, \tag{121}$$

where the effective density is given by

$$\rho^{*} = \rho + s\rho^{+}, \tag{122}$$

and the effective poroelastic constants are given by

$$c^{*}_{ijpq} = c_{ijpq} + s c^{+}_{ijkl} E_{klpq}, \tag{123}$$

$$\alpha^{*}_{ij} = \alpha\delta_{ij} + s\alpha^{+} E_{kkij} \tag{124}$$

and

$$\beta^{*} = \beta + s\beta^{+} + s\frac{(\alpha^{+})^2}{\kappa^{+}}(1 - E_{kkpp}/3). \tag{125}$$

The resulting effective medium is orthorhombic. The model may be readily extended to the case of variable crack sizes and orientations via a weighted sum or integral, just as with the elastic problem (Tod 2001).

The effective dynamic operator $\boldsymbol{\mathcal{L}}^*$ may be decomposed into four terms

$$\boldsymbol{\mathcal{L}}^* = \boldsymbol{\mathcal{L}}^0 + \boldsymbol{\mathcal{L}}^{\mathrm{p}} + s\boldsymbol{\mathcal{L}}^{\mathrm{c}} + s\boldsymbol{\mathcal{L}}^{\mathrm{p\&c}}, \tag{126}$$

where the first two terms are given by eqs (80) and (81) and

$$\mathcal{L}^{\mathrm{c}}_{ij} = \begin{pmatrix} c^{s+}_{ipkr} E_{krjq} \partial_p \partial_q + \rho_{\mathrm{s}}^{+} \omega^2 \delta_{ij} & 0 \\ 0 & 0 \end{pmatrix} \tag{127}$$

and

$$\mathcal{L}^{\mathrm{p\&c}}_{ij} = \begin{pmatrix} -c^{p+}_{ipkr} E_{krjq} \partial_p \partial_q + \left[\phi^{+} \rho_{\mathrm{f}} - (\phi \rho_{\mathrm{s}})^{+} + \rho_{\mathrm{f}}^2 \omega^2 \theta^{+}\right] \omega^2 \delta_{ij} & -\left[\alpha^{+} E_{kkip} + \rho_{\mathrm{f}} \omega^2 \theta^{+} \delta_{ip}\right] \partial_p \\ -\left[\alpha^{+} E_{kkiq} + \rho_{\mathrm{f}} \omega^2 \theta^{+} \delta_{ip}\right] \partial_q & \theta^{+} \nabla^2 - \beta^{+} - \dfrac{(\alpha^{+})^2}{\kappa^{+}} (1 - E_{kkpp}/3) \end{pmatrix}, \tag{128}$$

where $\boldsymbol{\mathcal{L}}^{\mathrm{c}}$ represents the contributions from the cracks and is identical to the result of Hudson (1994) and $\boldsymbol{\mathcal{L}}^{\mathrm{p\&c}}$ represents the interaction between the cracks and the pores, where the + superscript continues to represent the difference between a value in the poroelastic medium within the crack and that in the surrounding matrix. As the porosity in both materials vanish we return to the purely elastic problem (Hudson 1994).

As a result of the presence of anisotropy, solution of the governing equations becomes that much harder; not only are there now four distinct wave speeds, but the fluid pressure is no longer decoupled from the shear waves; the waves are no longer of pure-compressional or pure-shear type, but of a mixed nature. Using the fact that the mean wave is a plane wave allows us to write the poroelastic equivalent to both the Christoffel equation and the dispersion relation; the wave speeds of the four resultant waves may be found by solving

$$\det \begin{pmatrix} \mathring{\rho}^* \omega^2 \delta_{ip} - c^*_{ijpq} k_j k_q & -\mathrm{i}\mathring{\alpha}^*_{ij} k_j \\ -\mathrm{i}\mathring{\alpha}^*_{pj} k_j & -\theta^* k^2 - \beta^* \end{pmatrix} = 0. \tag{129}$$

8 DISCUSSION

As an example solution, we consider a poroelastic medium with the properties given earlier (Section 3) with a set of vertically aligned cracks filled with the same sandstone at a high (unconsolidated) porosity. We use, $\phi' = 0.8$ and thus $\alpha' = 1.0$, $\varsigma' = 1.0$, $m' = 1.1$ and $K' = 102.4\ \mu\mathrm{m}^2$, with the same fluid properties for the brine as in the matrix. We let the cracks have radii a, b and c, such that $a \geq b \geq c$, in the x_2, x_3 and x_1 directions, respectively, with aspect ratios $c/a = 0.005$ and $b/a = 0.5$.

The presence of the cracks reduces the speeds of the three fast waves, as with the elastic problem, but increases the speed of the Biot wave. In Fig. 1 the Biot wave speed is shown for the uncracked case and for crack volume densities of $s = 0.001$, 0.002 and 0.003, at vertical incidence. The increase in Biot wave speed is a result of increased energy dissipation into the fluid due to the scattering of waves by the cracks.

As with the uncracked case, the faster waves show negligible change in speed, and thus in anisotropy, with frequency, over the seismic bandwidth, and a similarly small change in speeds right up to the MHz range—by which point the approximations of the internal wavefield in terms of the external one will have broken down.

The shear wave speeds as a function of offset (i.e. the polar angle θ) at incidence inline with the smallest dimension of the crack size are shown in Fig. 2 for a crack volume density of $s = 0.003$. One of the shear waves, the quasi-*SH* wave, shows a 2θ variation, while the second, the quasi-*SV* wave, shows a 4θ variation, albeit a very small variation.

The shear wave anisotropy, Thomen's γ—the difference between the wave speed of the quasi-*SH* wave at vertical ($\theta = 0^\circ$) and horizontal incidence, scaled by the vertical wave speed—is considerable at 12.8 per cent and will scale roughly proportionally to the crack volume density. A shear wave singularity occurs at around 79°; at lower anisotropy this singularity will occur closer to the vertical. That the two shear

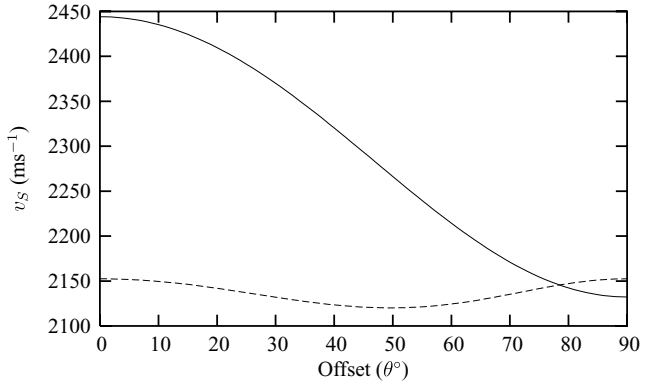

Figure 2. Variation in horizontal (solid line) and vertical (long dashes) shear wave speeds with offset angle at a crack volume density of 0.003.

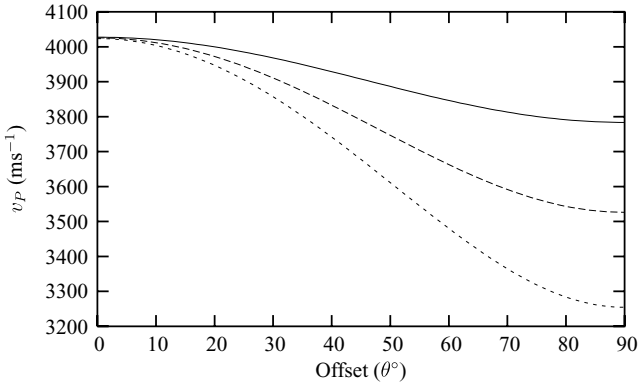

Figure 3. Variation in compressional wave speeds with offset angle at crack volume densities of 0.001 (solid line), 0.002 (long dashes) and 0.003 (short dashes).

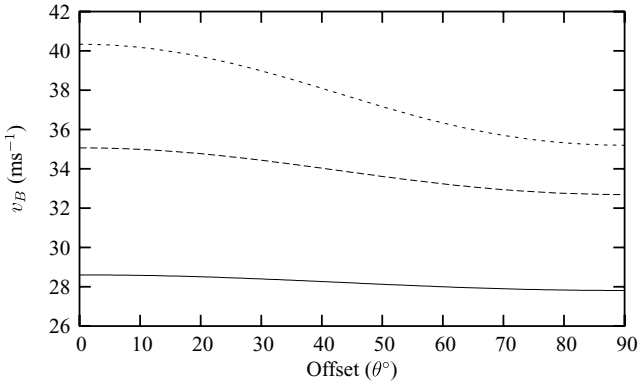

Figure 4. Variation in Biot wave speeds with offset angle at crack densities of $s = 0.001$ (solid line), 0.002 (long dashes) and 0.003 (short dashes).

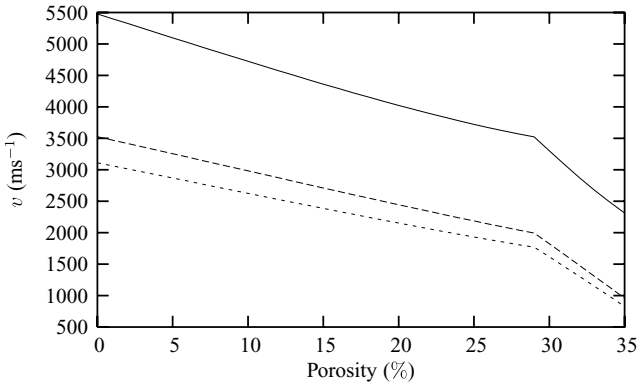

Figure 5. Variation in compressional (solid line) and shear (long and short dashes) wave speeds with matrix porosity.

wave speeds do not coincide exactly at horizontal incidence is a result of the medium being orthorhombic rather transversely isotropic; the aspect ratio of crack lengths $b/a = 0.5$ rather than unity.

Compressional wave speeds at densities of $s = 0.001$, 0.002 and 0.003, at the same inline incidence angle as in the shear case, are shown in Fig. 3. The (quasi-)compressional wave exhibits a 2θ variation. Again, the anisotropy, Thomsen's ϵ—the difference between the wave speed at vertical and horizontal incidence, scaled by the vertical wave speed—scales roughly as s, 6.1, 12.4 and 19.1 per cent for the three volume densities, respectively. The higher anisotropy associated with the compressional wave than with the shear wave at identical crack volume densities indicates that it is more influenced by the presence of the cracks.

The Biot wave exhibits marginally lower anisotropy than the shear waves, see Fig. 4, an anisotropy of 2.8 per cent at $s = 0.001$, rising to 12.7 per cent at $s = 0.003$.

The effects of changes in the matrix porosity of the background media are shown in Fig. 5. The wave speeds of the three fast waves are all seen to decrease with matrix porosity as it reduces from the elastic limit through the consolidation porosity at $\phi_c = 0.29$ towards a state of suspension. Examining the two shear wave speeds, we see that the shear wave anisotropy reduces with the porosity increase.

9 CONCLUSIONS

The equations of poroelastodynamics can be presented in a manner that is comparable to the equations of elastodynamics, enabling the ready computation of Green's functions and the use of a reciprocal theorem to represent solutions to scattering problems. This has enabled us to use the method of smoothing (Keller 1964) and a poroelastic equivalent to the result of Eshelby (1957), due to Berryman (1997), to derive an effective medium theory for ellipsoidal cracks in an isotropic poroelastic matrix, equivalent to the formulation of Hudson (1994) for the elastic problem.

As far as I am aware this provides the first anisotropic poroelastic theory for the presence of cracks in a background medium providing an explicit dependence on the orientation, size and content of the cracks. This provides an extension to the work of Hudson (1980, 1981, 1994) to incorporate the full range of matrix porosities observed in sandstone reservoirs.

The use of the approximation of Berryman (1997) restricts the range of frequencies at which we can expect the results to be reasonable, to probably not much more than the seismic range. A comparison with a full numerical solution would provide the best test of the range of validity of the approximation.

As has been pointed out, the predictions of Biot theory fail to explain the level of dispersion observed in experiments (e.g. Winkler 1985; Berryman & Wang 2001; King & Marsden 2002) and the addition of aligned cracks to the background material has failed to account for this underprediction. This failure is almost certainly a result of the lack of a local fluid flow mechanism within Biot theory. To be able to fully explain the observed dispersion would require the addition of an equivalent mechanism to that introduced by Hudson *et al.* (1996) and developed further by Tod (2001, 2002, 2003) and Tod & Liu (2002). While the squirt flow mechanism of Mavko & Jizba (1991) might appear a suitable candidate, the attempt by Dvorkin & Nur (1993) to couple this to Biot theory (the so-called BISQ model) violates Gassmann (1951a). A more appropriate approach would perhaps be along the lines of the squirt flow theory of Endres & Knight (1997), or the non-linear approach of de la Cruz *et al.* (1993).

Nevertheless, despite the inability of the theory to explain the observed dispersion, the theory has far reaching applications, such as providing considerably more accurate models of high porosity sandstone reservoirs in the hydrocarbon industry than existing theories based on an elastic description, provided we appreciate the restriction of the theory to the seismic frequency band.

ACKNOWLEDGMENTS

The author would like to thank John A. Hudson at DAMTP, University of Cambridge and Enru Liu at the British Geological Survey for support and encouragement, and Jim Berryman, Lawrence Livermore National Laboratory, Livermore, CA, for a helpful discussion. The work was sponsored by the Natural Environment Research Council through project GST022305, as part of the thematic programme *Understanding the microto-macro behaviour of rock fluid systems* ($\mu 2M$) and is published with the permission of the Executive Director of the British Geological Survey (NERC).

REFERENCES

Aifantis, E.C., 1980. On Barenblatt's problem, *Lett. appl. Eng. Sci.,* **18,** 857–867.

Altay, G.A. & Dökmeci, M.C., 1998. A uniqueness theorem in Biot's poroelasticity theory, *Z. angew. Math. Phys.,* **49,** 838–846.

Auriault, J.-L., 1980. Dynamic behaviour of a porous medium saturated by a Newtonian fluid, *Int. J. Eng. Sci.,* **18,** 775–785.

Auriault, J.-L., 1991. Heterogeneous medium. Is an equivalent macroscopic description possible?, *Int. J. Eng. Sci.,* **29,** 785–795.

Auriault, J.L. & Boutin, C., 1992. Deformable porous media with double porosity. Quasi-statics—I: Coupling effects, *Transp. Por. Med.,* **7,** 63–82.

Auriault, J.L. & Boutin, C., 1993. Deformable porous media with double porosity. Quasi-statics—II: Memory effects, *Transp. Por. Med.,* **10,** 153–169.

Auriault, J.L. & Boutin, C., 1994. Deformable porous media with double porosity—III: Acoustics, *Transp. Por. Med.,* **14,** 143–162.

Auriault, J.-L. & Royer, P., 2002. Seismic waves in fractured porous media, *Geophysics,* **67,** 259–263.

Barenblatt, G.I., Zheltov, Y.P. & Kochina, I.N., 1960. Basic concepts in the theory of seepage of homogeneous liquids in fissured rocks, *Priklad. Math. Mekhan.,* **24,** 852–864.

Batzle, M. & Wang, Z., 1992. Seismic properties of pore fluids, *Geophysics,* **57,** 1396–1408.

Berge, P.A., Fryer, G.F. & Wilkens, R.H., 1992. Velocity–porosity relationships in the upper oceanic crust: theoretical considerations, *J. geophys. Res.,* **97,** 15 239–15 254.

Berryman, J.G., 1981a. Elastic wave propagation in fluid-saturated porous media, *J. acoust. Soc. Am.,* **69,** 416–424.

Berryman, J.G., 1981b. Elastic wave propagation in fluid-saturated porous media II, *J. acoust. Soc. Am.,* **70,** 1754–1756.

Berryman, J.G., 1985. Scattering by a spherical inhomogeneity in a fluid-saturated porous medium, *J. Math. Phys.,* **26,** 1408–1419.

Berryman, J.G., 1986. Effective medium approximation for elastic constants of porous solids with microscopic heterogeneity, *J. appl. Phys.,* **59,** 1136–1140.

Berryman, J.G., 1997. Generalization of Eshelby's formula for a single ellipsoidal elastic inclusion to poroelasticity and thermoelasticity, *Phys. Rev. Lett.,* **79,** 1142–1145.

Berryman, J.G., 1998. Rocks as poroelastic composites, in *Poromechanics,* pp. 11–16, eds Thimus, J., Abousleiman, Y., Cheng, A.-D., Coussy, O. & Detournay, E., Balkema, Rotterdam.

Berryman, J.G. & Wang, H.F., 2000. Elastic wave propagation and attenuation in a double-porosity dual-permeability medium, *Int. J. Rock Mech. Min. Sci.,* **37,** 63–78.

Berryman, J.G. & Wang, H.F., 2001. Dispersion in poroelastic systems, *Phys. Rev. E,* **64,** 10.1103/PhysRevE.64.011303.

Biot, M.A., 1941. General theory of three-dimensional consolidation, *J. appl. Phys.,* **12,** 155–164.

Biot, M.A., 1955. Theory of elasticity and consolidation for a porous anisotropic solid, *J. appl. Phys.,* **26,** 182–185.

Biot, M.A., 1956. Theory of propagation of elastic waves in a fluid-saturated porous solid—II. Higher frequency range, *J. acoust. Soc. Am.,* **28,** 179–191.

Biot, M.A., 1962a. Mechanics of deformation and acoustic propagation in acoustic media, *J. appl. Phys.,* **33,** 1482–1498.

Biot, M.A., 1962b. Generalized theory of acoustic propagation in porous dissipative media, *J. acoust. Soc. Am.,* **34,** 1254–1264.

Boutin, C., Bonnett, G. & Bard, P.Y., 1987. Green functions and associated sources in infinite and stratified poroelastic media, *Geophys. J. R. astr. Soc.,* **90,** 521–550.

Brown, R.J.S. & Korringa, J., 1975. On the dependence of the elastic properties of a porous rock on the compressibility of the pore fluid, *Geophysics,* **40,** 608–616.

Burridge, R. & Keller, J.B., 1981. Poroelasticity equations derived from microstructure, *J. acoust. Soc. Am.,* **70,** 1140–1146.

Burridge, R. & Vargas, C.A., 1979. The fundamental solution in dynamic poroelasticity, *Geophys. J. R. astr. Soc.,* **58,** 61–90.

Chapman, M., Zatespin, S.V. & Crampin, S., 2002. Derivation of a microstructural poroelastic model, *Geophys. J. Int.,* **151,** 427–451.

Cheng, A.H.-D., 1997. Material coefficients of anisotropic poroelasticity, *Int. J. Rock Mech. Min. Sci.,* **34,** 199–205.

de la Cruz, V. & Spanos, T.J.T., 1985. Seismic wave propagation in a porous medium, *Geophysics,* **50,** 1556–1565.

de la Cruz, V. & Spanos, T.J.T., 1989. Thermomechanical coupling during seismic wave propagation in a porous medium, *J. geophys. Res.,* **94,** 637–642.

de la Cruz, V., Sahay, P.N. & Spanos, T.J., 1993. Thermodynamics of porous media, *Proc. R. Soc. Lond. A,* **443,** 247–255.

Deresiewicz, H. & Skalak, R., 1963. On uniqueness in dynamic poroelasticity, *Bull. seism. Soc. Am.,* **53,** 783–788.

Dvorkin, J. & Nur, A., 1993. Dynamic poroelasticity: a unified model with the squirt and Biot mechanisms, *Geophysics,* **58,** 524–533.

Endres, A.L. & Knight, R.J., 1997. Incorporating pore geometry and fluid pressure communication into modeling the elastic behavior of porous rocks, *Geophysics,* **62,** 106–117.

Eshelby, J.D., 1957. The determination of the elastic field of an ellipsoidal inclusion and related problems, *Proc. R. Soc. Lond. A,* **241,** 376–396.

Gassmann, F., 1951a. Über die Elastizität poröser Medien, *Vier. Natur. Gesell. Zurich,* **96,** 1–23.

Gassmann, F., 1951b. Elastic waves through a packing of spheres, *Geophysics,* **16,** 673–685.

Gist, G.A., 1994. Fluid effects on velocity and attenuation in sandstones, *J. acoust. Soc. Am.,* **96,** 1158–1173.

Hudson, J.A., 1980. Overall properties of a cracked solid, *Math. Proc. Camb. phil. Soc.,* **88,** 371–384.

Hudson, J.A., 1981. Wave speeds and attenuation of elastic waves in material containing cracks, *Geophys. J. R. astr. Soc.,* **64,** 133–150.

Hudson, J.A., 1994. Overall properties of materials with inclusions or cavities, *Geophys. J. Int.,* **117,** 555–561.

Hudson, J.A., Liu, E. & Crampin, S., 1996. The mechanical properties of materials with interconnected cracks and pores, *Geophys. J. Int.,* **124,** 105–112.

Johnson, D.L., Plona, T.J., Scala, C., Pasierb, F. & Kojima, H., 1982. Tortuosity and acoustic slow waves, *Phys. Rev. Lett.,* **49,** 1840–1844.

Kelder, O. & Smeulders, D.M.J., 1997. Observations of the Biot slow wave in water-saturated Nivelsteiner sandstone, *Geophysics,* **62,** 1794–1796.

Keller, J.B., 1964. Stochastic equations and wave propagation in random media, *Proc. Symp. appl. Math.,* **16,** 145–170.

King, M.S. & Marsden, J.R., 2002. Velocity dispersion between ultrasonic and seismic frequencies in brine-saturated reservoir sandstones, *Geophysics,* **67,** 254–258.

Korringa, J., 1981. On the Biot–Gassmann equations for the elastic moduli of porous rocks (Critical comment on a paper by J.G. Berryman), *J. acoust. Soc. Am.,* **70,** 1752–1753.

Kümpel, H.-J., 1991. Poroelasticity: parameters reviewed, *Geophys. J. Int.,* **105,** 783–799.

Kupradze, V.D., 1979. *Three-dimensional Problems of the Mathematical Theory of Elasticity and Thermoelasticity,* North-Holland, Amsterdam.

Kuster, G.T. & Toksöz, M.N., 1974. Velocity and attenuation of seismic waves in two-phase media: Part 1. Theoretical formulations, *Geophysics,* **39,** 587–606.

Le Ravalec, M. & Guéguen, Y., 1994. Permeability models for heated saturated igneous rocks, *J. geophys. Res.,* **99,** 24 251–24 261.

Le Ravalec, M. & Guéguen, Y., 1996. High- and low-frequency elastic moduli for a saturated porous/cracked rock—differential self-consistent and poroelastic theories, *Geophysics,* **61,** 1080–1094.

Levy, T., 1979. Propagation of waves in a fluid-saturated porous elastic solid, *Int. J. Eng. Sci.,* **17,** 1005–1014.

Manolis, G.D. & Beskos, D.E., 1989. Integral formulation and fundamental solutions of dynamic poroelasticity and thermoelasticity, *Act. Mech.,* **76,** 89–104.

Mavko, G.M. & Jizba, D., 1991. Estimating the grain-scale fluid effects on velocity dispersion in rocks, *Geophysics,* **56,** 1940–1949.

Mavko, G.M. & Nur, A., 1975. Melt squirt in the asthenosphere, *J. geophys. Res.,* **80,** 1444–1448.

Murphy, W., Reischer, A. & Hsu, K., 1993. Modulus decomposition of compressional and shear velocities in sand bodies, *Geophysics,* **58,** 227–239.

Nishizawa, O., 1982. Seismic velocity anisotropy in a medium containing orientated cracks—transversely isotropic case, *J. Phys. Earth,* **30,** 331–347.

Norris, A.N., 1985. A differential scheme for the effective moduli of composites, *Mech. Mater.,* **4,** 1–16.

O'Connell, R.J. & Budiansky, B., 1974. Seismic velocities in dry and saturated cracked solids, *J. geophys. Res.,* **79,** 5412–5426.

Plona, T.J., 1980. Observations of a second bulk compressional wave in a porous medium at ultrasonic frequencies, *Appl. Rev. Lett.,* **36,** 259–261.

Prasad, M., 2003. Velocity–permeability relations within hydraulic units, *Geophysics,* **68,** 108–117.

Pride, S.R., Gangi, A.F. & Morgan, F.D., 1992. Deriving the equations of motion for porous isotropic media, *J. acoust. Soc. Am.,* **92,** 3278–3290.

Rasolofosaon, P.N.J. & Zinszner, B.E., 2002. Comparison between permeability anisotropy and elasticity anisotropy of reservoir rocks, *Geophysics,* **67,** 230–240.

Sahay, P.N., 2001. Dynamic Green's function for homogeneous and isotropic porous media, *Geophys. J. Int.,* **147,** 622–629.

Schanz, M., 2001. Applications of 3D time domain boundary element formulation to wave propagation in poroelastic solids, *Eng. Anal. Bound. Elem.,* **25,** 363–376.

Seeburger, D.A. & Nur, A., 1984. A pore space model for rock permeability and bulk modulus, *J. geophys. Res.,* **89,** 527–536.

Thomsen, L., 1995. Elastic anisotropy due to aligned cracks in porous rock, *Geophys. Prospect.,* **43,** 805–829.

Tod, S.R., 2001. The effects on seismic waves of interconnected nearly aligned cracks, *Geophys. J. Int.,* **146,** 249–263.

Tod, S.R., 2002. The effects of stress and fluid pressure on the anisotropy of interconnected cracks, *Geophys. J. Int.,* **149,** 149–156.

Tod, S.R., 2003. Bed-limited cracks in effective medium theory, *Geophys. J. Int.,* **152,** 344–352.

Tod, S.R. & Liu, E., 2002. Frequency-dependent anisotropy due to fluid flow in bed limited cracks, *Geophys. Res. Lett.,* **29,** 10.1029/2002GL015369.

Vernik, L., 1998. Acoustic velocity and porosity systematics in siliciclastics, *Log Analyst,* **39,** 27–35.

Wilson, R.K. & Aifantis, E.C., 1984. A double porosity model for acoustic wave propagation in fractured–porous rock, *Int. J. Eng. Sci.,* **22,** 1209–1217.

Winkler, K.W., 1985. Dispersion analysis of velocity and attenuation in Berea sandstone, *J. geophys. Res.,* **90,** 6793–6800.

Yielding, G., Walsh, J. & Watterson, J., 1992. The prediction of small scale faulting in reservoirs, *First Break,* **10,** 449–460.

Zimmerman, R.W., 2000. Coupling in poroelasticity and thermoelasticity, *Int. J. Rock Mech. Min. Sci.,* **37,** 79–87.